Translation-rotation decoupling and nonexponentiality in room temperature ionic liquids

Philip J. Griffin,[1] Alexander L. Agapov,[2] and Alexei P. Sokolov[1,2,3]

[1]*Department of Physics and Astronomy, University of Tennessee, Knoxville, Tennessee 37996-1600, USA*
[2]*Department of Chemistry, University of Tennessee, Knoxville, Tennessee 37996-1600, USA*
[3]*Chemical Sciences Division, Oak Ridge National Laboratory, Oak Ridge, Tennessee 37830-6197, USA*

Using a combination of light scattering techniques and broadband dielectric spectroscopy, we have measured the temperature dependence of structural relaxation time and self diffusion in three imidazolium-based room temperature ionic liquids: [bmim][NTf$_2$], [bmim][PF$_6$], and [bmim][TFA]. A detailed analysis of the results demonstrates that self diffusion decouples from structural relaxation in these systems as the temperature is decreased toward T_g. The degree to which the dynamics are decoupled, however, is shown to be surprisingly weak when compared to other supercooled liquids of similar fragility. In addition to the weak decoupling, we demonstrate that the temperature dependence of the structural relaxation time in all three liquids can be well described by a single Vogel-Fulcher-Tamann function over 13 decades in time from 10^{-11} s up to 10^2 s. Furthermore, the stretching of the structural relaxation is shown to be temperature independent over the same range of time scales, i.e., time temperature superposition is valid for these ionic liquids from far above the melting point down to the glass transition temperature. We suggest that these phenomena are interconnected and all result from the same underlying mechanism—strong and directional intermolecular interactions.

I. INTRODUCTION

The molecular dynamics and structural relaxation in supercooled molecular liquids is an inherently complex and many-body process. This complexity is evident in the non-Arrhenius temperature dependence of dynamical processes, the nonexponentiality of the structural relaxation process, dynamical heterogeneity, and decoupling of translational and rotational motions. These unique features not only are found in the dynamics of supercooled molecular liquids [1–4], but also can be found in other disordered systems, such as spin glasses [5–7], relaxor ferroelectrics [8], bulk metallic glasses [9,10], and polymers [11–13]. Thus, to understand these phenomena in one class of systems will lead to a better understanding of dynamics in disordered systems in general.

The class of systems known as room temperature ionic liquids (RTILs) has recently been the subject of intense experimental and theoretical studies. They are incredibly useful materials in the fields of "green" chemistry and energy storage because of their nearly nonexistent vapor pressure, high levels of dc conductivity, and relatively large electrochemical window [14,15]. Recent studies of RTILs suggest that these materials, in general, exhibit characteristics that are very similar to those of prototypical molecular glass formers. They are easily supercooled, they exhibit non-Arrhenius temperature dependence of their transport properties [16], their structure is highly disordered [17], and they exhibit characteristic features in the dynamic susceptibility, such as the boson peak [18]. The RTILs are, thus, a suitable test bed in which to study dynamics in glass-forming systems in general. Furthermore, they are even better suited for these studies because it is possible to characterize the structural relaxation process via spectroscopic techniques as well as the self diffusion process via conductivity measurements.

In this paper, we present experimental studies of the temperature dependence of the structural relaxation and self diffusion processes in three imidazolium-based RTILs, [bmim][NTf$_2$], [bmim][PF$_6$], and [bmim][TFA]. We demonstrate that, in these liquids, the diffusion process decouples from the structural relaxation process as the temperature of the liquid decreases toward T_g, but the strength of the decoupling is found to be surprisingly weak. We also show that both the self diffusion rates and the structural relaxation times for these systems can be well described by single Vogel-Fulcher-Tamann (VFT) functions in the entire studied range (τ_α from $\sim 10^{-11}$ s up to 10^2 s), and no sign of a dynamic crossover appears in the derivative analysis of structural relaxation or diffusion (Stickel plot). This behavior is unlike that of nearly all fragile glass formers where the structural relaxation time exhibits a transition from one VFT behavior to another, usually at time scales of approximately 10^{-7} s. In addition to the absence of a change in temperature dependence of the transport processes, we demonstrate that the degree of nonexponentiality (as embodied in the stretching parameter) of the structural relaxation process in these RTILs is temperature independent from above the melting point down to T_g, i.e., time temperature superposition holds for the dynamics of these systems. We suggest that these experimental results are inherently connected to one another and that the intermolecular interactions are directly responsible for these experimentally observed phenomena.

II. EXPERIMENT

All measurements reported herein were performed on samples of 1-butyl-3-methylimidazolium hexafluorophosphate, [bmim][PF$_6$], and 1-butyl-3-methylimidazolium trifluoroacetate, [bmim][TFA], which were purchased from Sigma-Aldrich. All measurements performed on [bmim][NTf$_2$] have been previously reported in Ref. [19]. Prior to measurement, the samples were filtered through 0.22 micron polyvinylidene difluoride filters into clean, dry, cylindrical glass vials to remove any particulate contaminants from the liquid samples. Following filtration, the samples were placed into a vacuum

oven for 24 h at 350 K to remove any excess water or dissolved gasses. The samples were then removed from vacuum and were quickly sealed under ambient conditions.

Depolarized dynamic light scattering (DDLS) spectra were measured for both samples to characterize the structural relaxation process (α process) over 13 decades in time from 10^{-11} s through 100 s. For both ionic liquids, this corresponds to temperatures ranging from 375 K down to approximately 185 K, i.e., from above the melting point down to T_g. To characterize the α process at short time scales (10^{-11} s through 10^{-9} s), frequency domain measurements were performed in the backscattering geometry with laser wavelength $=532$ nm and laser power $=100$ mW using a Jobin Yvon T64000 triple monochromator spectrometer and a tandem Fabry-Pérot interferometer (Sandercock model) at three different free spectral ranges (10, 50, and 375 GHz). Interference filters were used to suppress higher order transmissions by the interferometer. By combining these two techniques, the depolarized light scattering intensity was measured in the frequency window of 0.5 GHz–10 THz. To characterize the α process at longer time scales (10^{-7} s through 100 s), depolarized photon correlation spectroscopy (PCS) measurements were performed in right angle geometry with laser wavelength $=647$ nm and laser power $=100$ mW. The scattered light was collected with a single mode optical fiber, was split between two avalanche photodiode detectors, and was cross correlated using an ALV-7004/FAST multi-τ digital correlator. All frequency domain light scattering measurements were performed with the sample mounted in a Janis ST-100 optical cryostat with temperature stability of ±0.5 K. All PCS measurements were performed with the sample mounted in an Oxford Optistat cryostat with temperature stability of ±0.1 K.

In addition to the light scattering measurements, broadband dielectric spectroscopy (BDS) was used to characterize the dc conductivity and ionic diffusion process for both systems over the similar range of temperatures as measured with DDLS. These measurements were performed using a Novocontrol Alpha-A impedance analyzer in the frequency window of 10^{-2} Hz–1 MHz. The samples were mounted in an upright cylindrical sample cell (BDS 1307) supplied by Novocontrol, GmbH. A Novocontrol Quattro temperature control unit was used to heat and to cool the sample with temperature stability of ±0.1 K.

III. RESULTS

A. Depolarized light scattering

For both [bmim][PF$_6$] ($T_g = 191$ K) and [bmim][TFA] ($T_g = 186$ K), DDLS spectra were measured in the temperature range of 295–375 K to characterize the α-relaxation process in the nanosecond-picosecond regime. The measured frequency dependent light scattering intensity was converted, by means of the fluctuation-dissipation theorem, into the imaginary part of the light scattering susceptibility, i.e., $\chi''(\omega) = I(\omega)/[n(\omega) + 1]$, where $I(\omega)$ is the measured intensity and $n(\omega) = [\exp(\frac{\hbar\omega}{kT}) - 1]^{-1}$ is the Bose factor. Figure 1 shows the measured susceptibility spectra in this temperature range for [bmim][TFA]. The susceptibility spectra for [bmim][PF$_6$] have very similar features and are not shown for the sake of brevity. At high temperatures, the peak of the α process enters
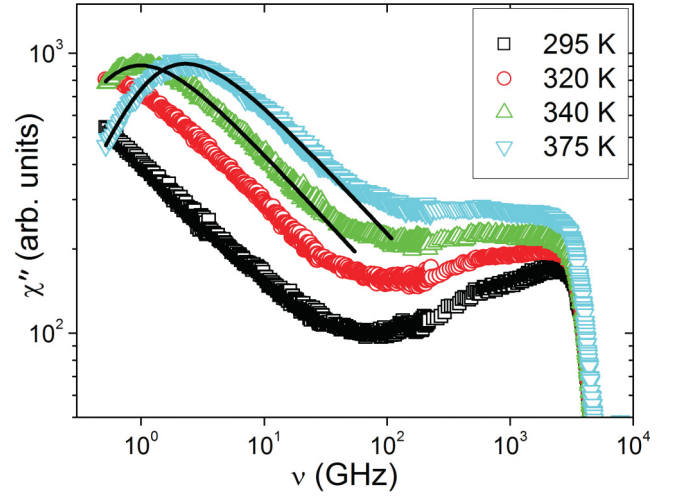

FIG. 1. (Color online) The imaginary part of the depolarized light scattering susceptibility of [bmim][TFA] at several temperatures. The solid lines are Cole-Davidson fits [Eq. (1)] of the main peak in the susceptibility spectrum corresponding to the α-relaxation process.

the frequency window of the spectrometer (at frequencies of 1–10 GHz in Fig. 1). The α process is accompanied by a weak spectral feature between 100 and 1000 GHz (boson peak vibrations) as well as the microscopic vibrational band at approximately 3–5 THz.

At temperatures where the α peak was visible in the susceptibility spectrum, this spectral feature was fit with the imaginary part of the Cole-Davidson function,

$$\chi''(\omega) = \chi_0\{\cos[\text{atan}(\omega\tau_{CD})]^\beta\}\sin[\beta_{CD}\,\text{atan}(\omega\tau_{CD})], \quad (1)$$

to determine the characteristic relaxation time and stretching parameter of the α process at a given temperature. τ_{CD} was converted to the most probable (peak) relaxation time τ_α via Eq. (2) [20],

$$\tau_\alpha = \frac{\tau_{CD}}{\tan\left(\frac{\pi}{2\beta_{CD}+2}\right)}, \quad (2)$$

and the empirical relationship between the Kohlrausch and the Cole-Davidson exponents derived by Lindsey and Patterson was used to convert β_{CD} to β_{KWW} [21]. Within this temperature range, corresponding to relaxation times of nanoseconds to picoseconds, the stretching parameter β_{KWW} was found to be independent of temperature in both systems with $\beta_{KWW} = 0.63 \pm 0.02$ for [bmim][PF$_6$] and $\beta_{KWW} = 0.61 \pm 0.02$ for [bmim][TFA].

PCS measurements were performed on both [bmim][PF$_6$] and [bmim][TFA] in the temperature range of 185–250 K to characterize the α process at longer relaxation times from 10^{-7} s through 100 s. Figure 2 shows the normalized ICFs for [bmim][TFA] at temperatures ranging from 190 to 230 K. The data for [bmim][PF$_6$] exhibit features very similar to those seen in Fig. 2. As is seen from Fig. 2, the primary decay in the ICF occurs at longer times as the temperature of the system is lowered toward T_g, but the overall shape of the ICF is independent of temperature. The primary decay in the ICF was fit using the Kohlrausch-Williams-Watts (KWW)
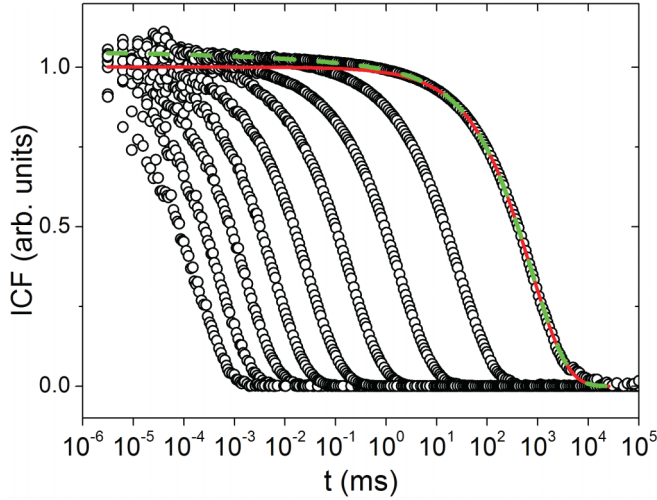
FIG. 2. (Color online) Normalized intensity correlation functions (ICFs) of [bmim][TFA] obtained by depolarized photon correlation spectroscopy. From left to right, the ICFs were recorded at 230, 225, 220, 215, 210, 205, 200, 195, and 190 K. The solid line is a fit of only the primary decay in the ICF at 190 K to the KWW relaxation function [Eq. (3)], and the dashed line is a fit of the entire data range at 190 K to a superposition of two KWW functions.

stretched exponential function,

$$\frac{\langle I(0)I(t)\rangle}{\langle I^2\rangle} - 1 = g_2(t) - 1 = \varphi|g_1(t)|^2$$

$$= \varphi\left\{\exp\left[-\left(\frac{t}{\tau_{\text{KWW}}}\right)^\beta\right]\right\}^2. \quad (3)$$

Fitting this subset of ICF data to Eq. (3), one obtains the spatial coherence factor of the primary decay φ, the characteristic decay time τ_{KWW}, and the nonexponentiality parameter β_{KWW}. The spatial coherence factor φ was quite sensitive to alignment of the sample and external optical elements and was found to be approximately $\varphi = 0.4$ for [bmim][PF$_6$] and $\varphi = 0.65$ for [bmim][TFA]. The stretching parameter as determined by Eq. (3) for [bmim][PF$_6$] was $\beta_{\text{KWW}} = 0.61 \pm 0.02$, and for [bmim][TFA], the stretching parameter was $\beta_{\text{KWW}} = 0.62 \pm 0.02$ for all measured temperatures. The characteristic decay time τ_{KWW} was converted to the most probable relaxation time τ_α by numerically simulating the one-sided sine Fourier transform of the best fit KWW relaxation function [21]. The temperature dependent τ_α and β_{KWW} for the three RTILs are shown in Figs. 3 and 4, respectively, alongside the values obtained from frequency domain DDLS.

In addition to the main decay of the depolarized ICF, which can be attributed to the molecular reorientation or structural relaxation process in molecular liquids [22–25], the three RTILs presented in this paper also have a weak feature in the depolarized ICF that appears as an additional step superimposed on top of the α decay. This feature, which has been attributed to a secondary relaxation or excess wing in molecular liquids [25], appears in the ICF at low temperatures. It can also be seen in Fig. 2 of Ref. [19] that the high frequency flank of the α process in the light scattering susceptibility spectra of [bmim][NTf$_2$] becomes flattened as temperature
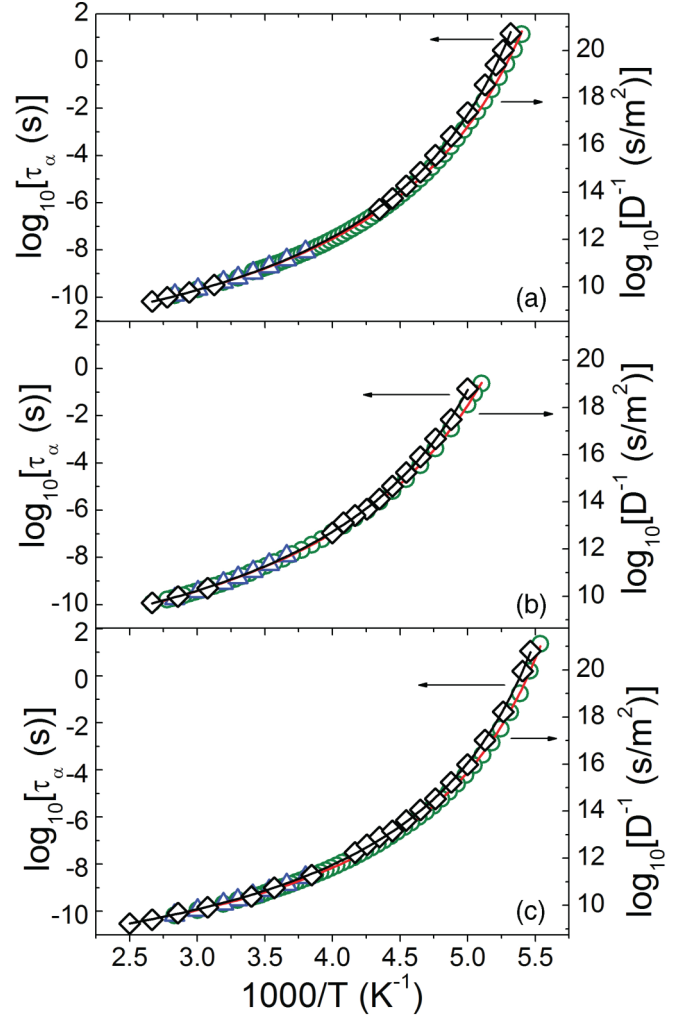

FIG. 3. (Color online) Open diamonds: temperature dependence of structural relaxation times; open circles: measured inverse diffusion coefficients; and open triangles: literature values of the inverse diffusion coefficient measured via pulsed field gradient NMR (PFG NMR) (Ref. [34]) for the three RTILs. (a) =[bmim][TFA], (b) =[bmim][PF$_6$], and (c) =[bmim][NTf$_2$]. Structural relaxation times correspond to the left axis, and inverse diffusion coefficients correspond to the right axis. The solid lines are VFT fits to light scattering relaxation times and the inverse diffusion coefficients.

decreases toward T_g, indicating the presence of the excess wing in the DDLS spectrum [18]. The comparison between the two different fitting functions in Fig. 5 clearly illustrates this additional relaxation process in the ICF data. Consequently, in order to accurately characterize the α process, one must take this excess relaxation component of the ICF into account and either fit only the main decay of the ICF or fit the entire data set with a superposition of two KWW functions. As can be seen in Fig. 5, both fitting methods yield identical reproduction of the data in the region of the α decay. In our previous article on [bmim][NTf$_2$] [19], we had overlooked this subtlety of the analysis of the ICF, and consequently, we erroneously reported the values for β_{KWW} as being weakly temperature dependent close to T_g. We have reanalyzed the ICF data for [bmim][NTf$_2$] in an identical fashion to the data reported herein, and we find the stretching parameter of the α process in [bmim][NTf$_2$]
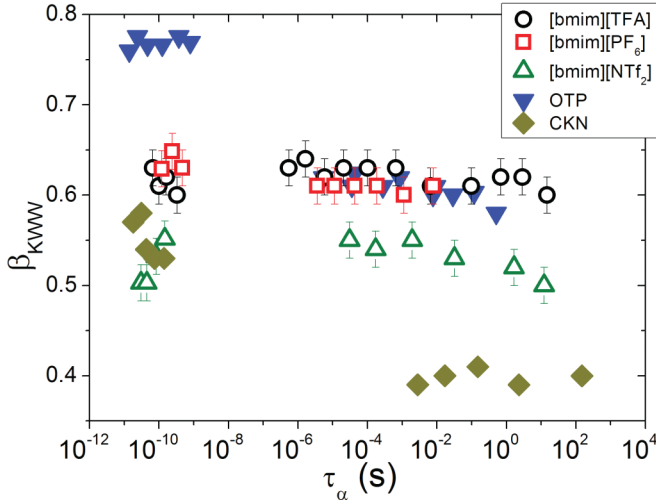
FIG. 4. (Color online) KWW stretching parameter vs τ_α for the three RTILs obtained from depolarized light scattering measurements of structural relaxation. The literature data for OTP [50] and Ca-K-(NO$_3$) were also obtained via depolarized light scattering. It can be clearly seen that the stretching parameter is independent of temperature in the RTILs from above the melting point down to T_g, whereas, it changes significantly in OTP and Ca-K-(NO$_3$). For Ca-K-(NO$_3$), the short time data are from Li *et al.* [51], and the long time data are from Sidebottom and Sorensen [49].

is temperature independent in the PCS time window with $\beta_{KWW} = 0.55 \pm 0.02$.

B. Dielectric spectroscopy

The frequency dependent dielectric response of [bmim][PF$_6$] and [bmim][TFA] was measured over the
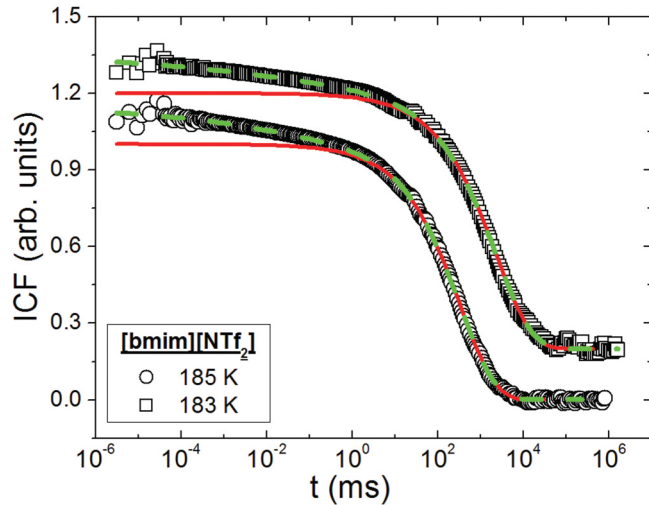

FIG. 5. (Color online) Two normalized intensity correlation functions for [bmim][NTf$_2$] at temperatures close to the glass transition ($T_g = 181$ K). The data at 183 K are offset by a constant $=0.2$ for clarity. The solid line is the KWW fit to the primary decay only, and the dashed line is the superposition fit described in the text. The additional fast process, possibly a signature of the excess wing, is clearly seen as an additional feature superimposed on top of the α-relaxation process.

temperature range of 185–375 K to characterize the ionic conductivity and diffusion process in these RTILs. Examples of dielectric spectra for [bmim][TFA] in complex permittivity and conductivity notations are shown in Fig. 6. The data were analyzed in the complex conductivity representation $\sigma^*(\omega) = i\omega\varepsilon_0\varepsilon^*(\omega)$. Conductivity spectra were fit with a sum of two processes. The first process was fit according to the Dyre model for ion transport $\sigma(\omega) = \sigma_0(\frac{i\omega\tau_e}{\ln(1+i\omega\tau_e)})$, where τ_e is the characteristic hopping time of an ion [26,27]. The second process appeared as a peak in ε'' and an additional step in ε' and was fit as a Cole-Cole process. The resulting fit function had the form

$$\sigma(\omega) = \sigma_0 \left(\frac{i\omega\tau_e}{\ln(1+i\omega\tau_e)} \right) + i\omega\varepsilon_0 \left(\varepsilon_\infty + \frac{\Delta\varepsilon}{1+(i\omega\tau_{cc})^\beta} \right).$$

(4)

The nature of the observed Cole-Cole process is not well understood. This Cole-Cole process for both ionic liquids showed very moderate stretching with $\beta \approx 0.70$–0.80 and was always positioned at the characteristic frequency region where $\varepsilon' \approx \varepsilon''$. The frequency at which $\varepsilon' = \varepsilon''$ defines the well known conductivity relaxation frequency [28] that appears as a peak in electric modulus representation $\omega_c = \frac{\sigma_0}{\varepsilon_\infty\varepsilon_0}$. However, for homogeneous materials, this conductivity relaxation should not have any peaklike contribution to the permittivity losses. It is possible that we observe structural dynamics of the ionic liquids in our dielectric spectra according to a recent paper where the mechanical structural relaxation rate for various ionic liquids coincides with the ω_c from dielectric measurements [29]. However, another recent paper demonstrated that the appearance of a Debye-like process in the dielectric spectra at frequencies where $\varepsilon' = \varepsilon''$ may be an artifact of the measurements due to insulating impurities present in the capacitor volume [30].

The Dyre model for ion conduction allows one to determine the characteristic diffusion rate of an ionic liquid as a function of temperature. In the framework of the Dyre model for ion transport, the ionic conductivity can be described as a random hopping process where the characteristic hopping rate is determined by a spatially heterogeneous energy landscape. The Dyre model has been shown to accurately describe the conductivity spectrum for numerous RTILs [31,32]. Furthermore, the Dyre model has also been shown to provide good quantitative predictions for the temperature dependence of the diffusion coefficient and the number density of free ions in RTILs [31,32]. At a given temperature, the main quantities that are extracted from the conductivity spectrum in this model are the ion hopping time τ_e and the dc conductivity σ_0. Using the Einstein-Smoluchowski relation ($D = \frac{\lambda^2}{2\tau_h}$) and the Nernst-Einstein relation ($\sigma_0 = n\frac{q^2D}{kT}$), the temperature dependence of the free ion concentration can be determined via Eq. (5),

$$\sigma_0 = n\frac{q^2}{kT}\frac{\lambda^2}{2\tau_h},$$

(5)

where the parameter τ_h is the hopping time of an ion, λ is the hopping length of the diffusing species (typically on the order of the Pauling diameter of an RTIL [33]), n is the free ion concentration, q is the ion charge, k is the Boltzmann constant, and T is temperature. The free ion concentration in the RTILs was
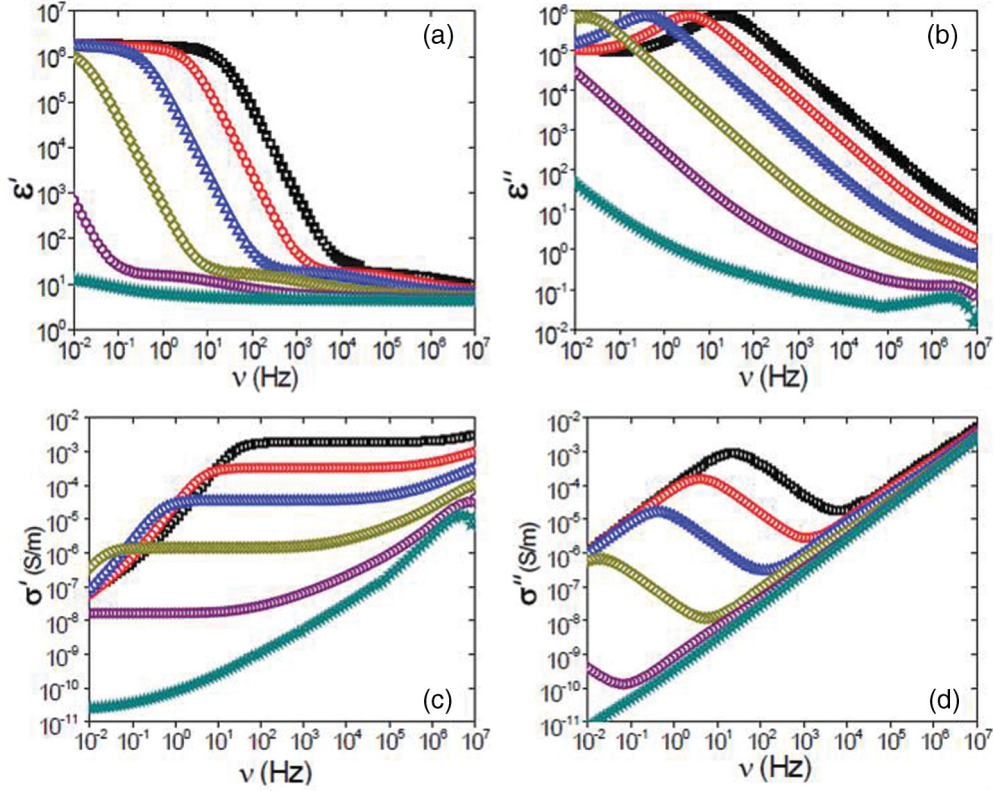
FIG. 6. (Color online) Dielectric spectra of [bmim][TFA] in complex permittivity notation (a) and (b) $\varepsilon = \varepsilon' - i\varepsilon''$ and complex conductivity notation (c) and (d) $\sigma = \sigma' + i\sigma''$ plotted as a function of frequency for different temperatures (squares: 235 K; circles: 225 K; triangles: 215 K; diamonds: 205 K; hexagons: 195 K; and stars: 185 K).

calculated via Eq. (5) assuming that $\tau_h \approx \tau_e$ and using $\lambda = 0.11$ and 0.14 nm for [bmim][TFA] and [bmim][PF$_6$], respectively. The free ion concentration was found to have Arrhenius temperature dependence over the entire experimentally available temperature range with [bmim][TFA] having activation energy $E_A = 0.022$ eV and [bmim][PF$_6$] having activation energy $E_A = 0.010$ eV. At high temperatures, determination of τ_h is not possible because it is out of the window of the spectrometer on the high frequency side. As a consequence, diffusion cannot be directly calculated with the Einstein-Smoluchowski relation. In order to determine the diffusion coefficient over the entire temperature range, the free ion concentration extrapolated to high temperatures (using the Arrhenius temperature dependence determined at lower temperature) and the measured dc conductivity were substituted back into the Nernst-Einstein relation to calculate diffusion at these higher temperatures.

From the above method, we have indirectly measured the temperature dependent diffusion coefficient in both [bmim][PF$_6$] and [bmim][TFA]. The results of this analysis are shown in Fig. 3 along with PFG NMR measurements of diffusion from the literature [34] and the results for structural relaxation time as measured via depolarized light scattering.

IV. DISCUSSION

A. Decoupling of ionic diffusion from structural relaxation

The temperature dependence of both ionic diffusion and structural relaxation is strongly non-Arrhenius for these three

imidazolium-based ionic liquids (Fig. 3) as is characteristic of most glass-forming liquids. To quantify the degree of deviation from Arrhenius temperature dependence, the fragility m is commonly used and is defined as

$$m = \left. \frac{d \, \log_{10} \tau_\alpha}{d \frac{T_g}{T}} \right|_{T=T_g}, \qquad (6)$$

where T_g is the glass transition temperature [35]. Defining T_g as the temperature at which the α-relaxation time is 100 s, we have calculated the fragility and T_g for each RTIL (for [bmim][PF$_6$], $m = 75$ and $T_g = 191$ K; for [bmim][TFA], $m = 80$ and $T_g = 186$ K; for [bmim][NTf$_2$], $m = 95$ and $T_g = 181$ K). As can be seen, an increase in anion size ([PF$_6$] < [TFA] < [NTf$_2$]) leads to a decrease in T_g and an increase in fragility. These results for the glass transition temperature agree with earlier studies on RTILs, which demonstrate that T_g decreases as the size of the cation or anion becomes larger [34,36,37]. We speculate that this size effect reduces Coulombic interactions between ion species, which, consequently, decreases T_g because of the decrease in cohesive energy [38]. The increase in fragility, on the other hand, is also related to the size of the ion. As the ion size increases, the molecular packing becomes increasingly frustrated, which generally leads to more fragile behavior of the liquid [39].

In Fig. 3, it is also seen that, for all three systems, the ionic diffusion process has slightly different temperature dependence than the corresponding α-relaxation process.

The diffusion process changes with temperature less quickly than the α-relaxation process. This phenomenon of enhanced diffusion, or decoupling of diffusion from structural relaxation, violates the Debye-Stokes-Einstein (DSE) and Stokes-Einstein (SE) relations and has been observed in numerous other glass-forming systems [1,40–43]. Decoupling effects have also been reported for the RTIL [bmim][PF$_6$] [18,44].

The DSE and SE relations predict that, in simple liquids, translational and rotational diffusion times are proportional to one another, and the proportionality constant is independent of temperature. Explicitly, the ratio $R = D\tau_\alpha$ should be constant with temperature. This ratio has been shown to hold at high temperatures from above the melting point down to the so-called crossover temperature T_C for many glass-forming liquids. It has been demonstrated for numerous glass-forming liquids, however, that the quantity R changes drastically at temperatures close to T_g (see Refs. [1,40–43]). To account for the temperature dependence of R, a fractional DSE relation was proposed in which the ratio R depended on the structural relaxation time via a power law, i.e., $R = D\tau_\alpha \propto \tau_\alpha^\varepsilon$, where ε characterized the degree to which the diffusion and structural relaxation were decoupled from one another [40–43]. For the glass former 1,3,5-tris-naphthyl-benzene (TNB), R changes by nearly 2 orders of magnitude from high temperature to T_g with $\varepsilon \approx 0.15$, and for ortho-terphenyl (OTP), R changes by 2 orders of magnitude with $\varepsilon \approx 0.25$ [43].

We have analyzed the decoupling of the diffusion and structural relaxation times in terms of the fractional DSE relation for the three RTILs (Fig. 7). The ratio R changes with relaxation time nearly identically for the three RTILs. It changes by less than 1 order of magnitude from high temperatures down to T_g, and the decoupling exponent ε is approximately 0.10 ± 0.01 for the three systems. From the recent paper of Sokolov and Schweizer [12], the decoupling exponent is expected to correlate to the fragility of the structural relaxation process. It is clear that this model does not account
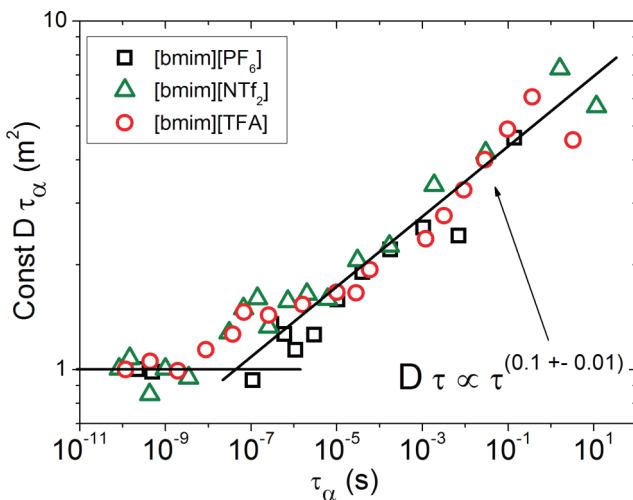

FIG. 7. (Color online) Normalized decoupling ratio R vs τ_α for the three RTILs. Data were normalized to one at high temperature. It is seen that, below $\tau_\alpha \approx 10^{-5}$ s, the decoupling ratio can be described in the form $R = D\tau_\alpha \propto \tau_\alpha^\varepsilon$ with the decoupling exponent ε equal to 0.1 ± 0.01 for each system. The line at larger τ_α's depicts this power law dependence.

for the fragility independent decoupling in the three RTILs. Perhaps most interesting is that the strength of decoupling, as characterized by ε, is unexpectedly weak for these systems when compared to other systems of similar fragility, such as OTP and Ca-K-(NO$_3$) where the decoupling exponents are approximately 0.25 and 0.35, respectively [19,41].

The precipitous change in the quantity R is thought to stem directly from the effects of dynamical heterogeneity in glass formers [45,46]. It is hypothesized that distinct regions of varying molecular mobility first form then begin to grow as a supercooled liquid is cooled toward T_g. These regions consist of dynamically correlated molecules, some of which are essentially frozen when compared to the average mobility of the distribution, whereas, some consist of highly liquidlike molecules. The structural relaxation time, when measured with a macroscopic probe, such as depolarized light scattering, is an ensemble average of all sampled relaxation times $\langle\tau\rangle$, whereas, the diffusion coefficient is an ensemble average of all sampled inverse relaxation times $\langle\tau^{-1}\rangle$. Thus, the measured α-relaxation time is heavily weighted by slow components of a distribution of relaxation times, whereas, the measured diffusion coefficient is heavily weighted by fast components of the distribution.

According to the barrier hopping theory of Schweizer and Saltzman [45], as a glass-forming liquid cools toward T_g, dynamical heterogeneity becomes increasingly prominent, the relaxation time distribution widens, and the gap between $\langle\tau\rangle$ and $\langle\tau^{-1}\rangle$ becomes more pronounced. Thus, the prominent conclusion of this theoretical framework is that temperature dependent decoupling of the structural relaxation time and diffusion coefficient is caused by a temperature dependent increase in the distribution of relaxation times, i.e., a temperature dependent stretching parameter β_{KWW}. This conclusion is problematic on a fundamental level, however. The glass formers OTP [47], TNB [48], and Ca-K-(NO$_3$) [49], for which decoupling effects are quite prevalent, have nearly temperature *independent* stretching of the α-relaxation process in the temperature range where decoupling is strong. As can be seen from Fig. 4, all three RTILs also have temperature independent stretching of the α-relaxation process. These examples conclusively show that there is no direct connection between the temperature dependence of the stretching of the α-relaxation process and the temperature dependence of translational-rotational decoupling in glass-forming liquids, contrary to the above stated dynamical heterogeneity hypothesis. However, it is very interesting that the observed temperature dependence of β_{KWW} in OTP [50] and Ca-K-(NO$_3$) [49,51] occurs primarily *before* the decoupling of diffusion and structural relaxation sets in and not alongside the decoupling phenomenon. This result suggests that temperature dependent stretching of the structural relaxation process might be a precursor to strong decoupling of translational and rotational degrees of freedom.

B. No change in temperature dependence of diffusion or structural relaxation

Usually associated with the decoupling effect and the onset of dynamical heterogeneity is the existence of two distinct regions of temperatures in which the structural relaxation time of a given glass-forming liquid exhibits considerably different temperature dependences. It has been shown that, in each
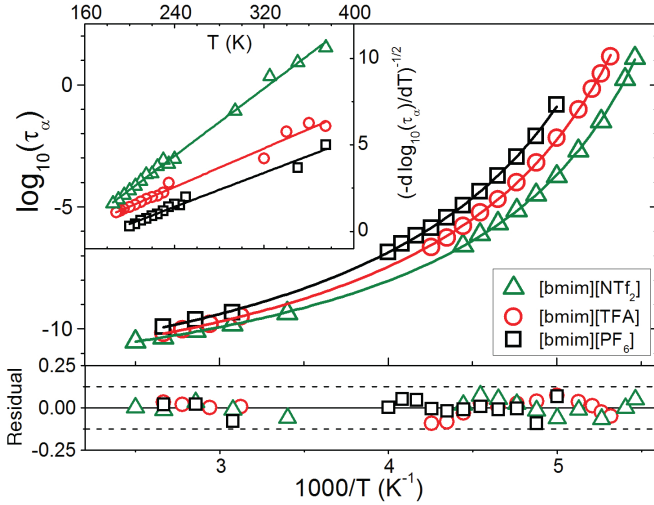
FIG. 8. (Color online) The main part of the figure shows the temperature dependence of $\log_{10}(\tau_\alpha)$ for the three RTILs with the corresponding solid lines presenting single VFT fits over the whole range of temperatures. The bottom subplot presents the residual (in $\log_{10}$ units) of each data set to the corresponding VFT fit. The maximum residual is ≈ 0.1 $\log_{10}$ units for any of the three systems. The upper left inset shows the Stickel derivative of the relaxation time measured via depolarized light scattering, and there is no indication of any change in temperature dependence.

of these two distinct regions, generally speaking, different VFT functions are required to describe the experimental data [52,53]. Stickel *et al.* proposed a derivative analysis of the temperature dependence of structural relaxation that can directly identify the existence of a change in temperature dependence of the structural relaxation time [52]. In Stickel's derivative analysis, a VFT function appears as a straight line in temperature with each VFT function defined by a characteristic slope. In the case of most fragile glass-forming liquids, the temperature dependence of a relaxation process usually changes from one VFT behavior to another at some crossover temperature T_B. This crossover temperature can be determined by locating the intersection of two straight lines of different slopes when analyzed with this derivative technique. It has been explicitly shown that, for those systems with a clear signature of a Stickel crossover, one VFT equation cannot accurately describe the temperature dependence of relaxation times [54].

We have analyzed the DDLS α-relaxation times and diffusion rates with the derivate technique of Stickel. From the inset of Fig. 8, it is clearly seen that there is no indication of a change in VFT temperature dependence of the α-relaxation time in any of the three RTILs. In order to more clearly show that this conclusion is correct, we have fit the α-relaxation times of the RTILs to single VFT functions over the entire temperature range (above T_{melting} down to T_g) (Fig. 8). The residuals of these least squares VFT fits oscillate randomly about zero for all three systems and are never larger than ± 0.1 $\log_{10}$ units. It is instructive to compare this result to the results of Casalini *et al.* in which deviations in the VFT fits over similar ranges of relaxation times are much larger and more systematic for systems that exhibit the crossover as determined by the derivative technique [54]. With this comparison, it is
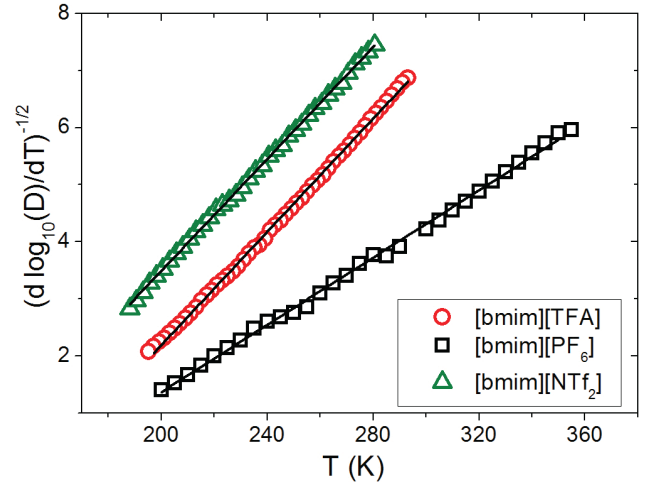

FIG. 9. (Color online) Stickel derivative analysis of self diffusion in the RTILs as determined from dielectric spectroscopy and analysis using the Dyre model. It can be seen that there is no indication of a change in temperature dependence in the self diffusion process.

clearly seen that the temperature dependence of the structural relaxation time in these RTILs is much different than other glass formers of similar fragility, such as OTP, salol, propylene carbonate, and Ca-K-(NO_3), which all show a clear crossover in the temperature dependence of their relaxation times.

Results obtained from the derivative analysis of diffusion rates as measured by dielectric spectroscopy are much more straightforward and conclusive than the results of the derivative analysis of DDLS (it is much quicker to acquire a dielectric spectrum than a depolarized light scattering spectrum, thus, it is possible to measure many more temperature points). In Fig. 9, it can be seen that there is also no indication of a change in temperature dependence in the diffusion process of any of these three RTILs.

C. Temperature independent stretching and weak decoupling

We have demonstrated above that the structural relaxation process decouples from the diffusion process in the three RTILs presented herein. This is to be expected, generally speaking, because numerous fragile glass formers show decoupling of translational and rotational motions as the temperature decreases toward T_g. However, it is also clear that the strength of decoupling, when compared to systems of similar fragility, is significantly lower than is expected. As stated previously, these RTILs have a decoupling parameter ε equal to 0.10 ± 0.01 for the three systems, whereas, OTP (fragility $m \approx 80$), for example, has been shown to exhibit a decoupling parameter ε approximately equal to 0.25 [41]. This is a very significant difference, but it can be rationalized by considering the following. In these RTILs, intermolecular interactions strongly influence the molecular dynamics. Clearly, RTILs are ionic systems, and Coulombic forces are certainly present in the interaction Hamiltonian. However, the Coulombic interactions are most probably not responsible for the weak decoupling in RTILs because the ionic glass-former Ca-K-(NO_3) exhibits exceptionally strong decoupling of translational and rotational motions ($\varepsilon \approx 0.35$) [19].

The other prominent intermolecular interaction inherent to these three RTILs is their propensity to form hydrogen bonds between cations and anions [55–57]. This hydrogen bonding provides a directional interaction between molecules and can serve as a link between the translational and rotational degrees of freedom. It is possible that, as structural relaxation occurs, the cation will execute reorientational motions that orient it preferentially toward a new hydrogen bonding site. The cation center of mass simultaneously translates by small steps through the liquid as it progressively makes and breaks hydrogen bonds with other molecules through the reorientation process. Based on this qualitative hypothesis, we speculate that the strong influence of the hydrogen bond in the molecular motion of these RTILs is responsible for the unusually weak decoupling of translational and rotational motion near T_g. Following this hypothesis, it is also possible to explain the absence of decoupling in the network oxide SiO_2 [12] because the intermolecular interactions present for the case of SiO_2 are purely covalent and, thus, strongly directional in nature.

We have shown that the stretching parameter is independent of temperature for all three RTILs (Fig. 4) from temperatures significantly above the melting point down to the glass transition temperature. In the Coupling Model, the stretching of the α process is caused by intermolecular interactions and many-body effects on the molecular dynamics [4]. The model states that the strength of this interaction can qualitatively be determined by quantifying how stretched the α process is, with a smaller β_{KWW} indicating stronger intermolecular coupling. However, the Coupling Model predicts that near some crossover temperature, a system should transition from a state of nearly independent molecular motion at high temperatures to a state of stronger molecular cooperativity at low temperatures. As is seen in Fig. 4, both OTP and Ca-K-(NO_3) exhibit this transition, whereas, the three RTILs clearly do not exhibit any change in β_{KWW}. From considering this result in the framework of the Coupling Model, it follows that the intermolecular interactions that control structural relaxation at low temperatures persist well above the melting point in these three RTILs.

Another explanation for the stretching of the structural relaxation is dynamic heterogeneity [1]. In this interpretation, our results would mean that there is no change in dynamic heterogeneity in the studied RTILs in the entire temperature range. Regardless of the interpretation of the stretching, it is tempting to relate the temperature dependence of β_{KWW} and the magnitude of decoupling when comparing the behavior of the RTILs, OTP, and Ca-K-(NO_3). We speculate that the absence of temperature dependence of the stretching parameter β_{KWW} might be directly connected to the experimentally observed weak decoupling of diffusion and structural relaxation in the RTILs.

V. CONCLUSION

We have measured the ionic diffusion and structural relaxation of two imidazolium-based room temperature ionic liquids [bmim][PF_6] and [bmim][TFA] in a broad temperature and frequency range. The detailed analysis of the results, in addition to results previously reported for [bmim][NTf_2], demonstrates that diffusion is decoupled from the structural relaxation process in all three materials, but the decoupling effect is significantly weaker than that observed in other glass-forming liquids of similar fragility. Specifically, the decoupling parameter ε was found to be approximately 0.1 for the three systems studied and is independent of fragility. From these results, it seems that *weak* decoupling is a generic feature of imidazolium-based ionic liquids. Contrary to previous assertions in the literature, it is feasible that the decoupling parameter ε is not correlated to the fragility m for other types of glass-forming liquids as well.

In addition to this result, we have demonstrated that the temperature dependence of diffusion and structural relaxation of these ionic liquids is well described with single VFT functions over a broad range of temperatures, corresponding to relaxation times of 10^{-11}–100 s. The single VFT temperature dependence of the structural relaxation time is also accompanied by a temperature independent stretching of the α process, i.e., time temperature superposition of the α process holds from above the melting point down to T_g in these materials. These unique features of the RTILs are quite different from the cases of other fragile liquids: For example, both OTP and Ca-K-(NO_3) exhibit changes in the stretching parameter, changes in VFT temperature dependence, and much larger decoupling effects.

The results of this paper demonstrate that temperature dependent decoupling of translational and rotational motions in supercooled liquids does not necessitate a *simultaneously* temperature dependent stretching of the primary structural relaxation process. Furthermore, the results of this paper suggest that the fragility of a system may not be the primary factor in determining the degree to which translational dynamics are decoupled from structural relaxation in glass-forming liquids. Instead, we suggest that the main determining factors might be the details of the intermolecular interactions, in particular, their directional character.

[1] M. D. Ediger, Annu. Rev. Phys. Chem. **51**, 99 (2000).

[2] J. C. Dyre, Rev. Mod. Phys. **78**, 953 (2006).

[3] C. A. Angell, K. L. Ngai, G. B. McKenna, P. F. McMillan, and S. W. Martin, J. Appl. Phys. **88**, 3113 (2000).

[4] K. L. Ngai, *Relaxation and Diffusion in Complex Systems* (Springer, New York, 2011).

[5] I. A. Campbell, J. M. Flesselles, R. Jullien, and R. Botet, Phys. Rev. B **37**, 3825 (1988).

[6] I. A. Campbell, A. Amato, F. N. Gygax, D. Herlach, A. Schenck, R. Cywinski, and S. H. Kilcoyne, Phys. Rev. Lett. **72**, 1291 (1994).

[7] D. L. Smith, H. J. Stapleton, and M. B. Weissman, Phys. Rev. B **33**, 7417 (1986).

[8] O. Kircher, B. Schiener, and R. Bohmer, Phys. Rev. Lett. **81**, 4520 (1998).

[9] A. Meyer, R. Busch, and H. Schober, Phys. Rev. Lett. **83**, 5027 (1999).

[10] L. M. Wang, R. P. Liu, and W. H. Wang, J. Chem. Phys. **128**, 164503 (2008).

[11] A. Arbe, Physica B **350**, 178 (2004).

[12] A. P. Sokolov and K. S. Schweizer, Phys. Rev. Lett. **102**, 248301 (2009).

[13] C. M. Roland, Macromolecules **43**, 7875 (2010).

[14] R. D. Rogers and K. R. Seddon, Science **302**, 792 (2003).

[15] M. Armand, F. Endres, D. R. MacFarlane, H. Ohno, and B. Scrosati, Nature Mater. **8**, 621 (2009).

[16] W. Xu, E. I. Cooper, and C. A. Angell, J. Phys. Chem. B **107**, 6170 (2003).

[17] A. Triolo *et al.*, J. Phys. Chem. B **110**, 21357 (2006).

[18] A. Rivera, A. Brodin, A. Pugachev, and E. A. Rossler, J. Chem. Phys. **126**, 114503 (2007).

[19] P. Griffin, A. L. Agapov, A. Kisliuk, X. G. Sun, S. Dai, V. N. Novikov, and A. P. Sokolov, J. Chem. Phys. **135**, 114509 (2011).

[20] F. Kremer and A. Schönhals, *Broadband Dielectric Spectroscopy* (Springer, Berlin/New York, 2003).

[21] C. P. Lindsey and G. D. Patterson, J. Chem. Phys. **73**, 3348 (1980).

[22] H. Z. Cummins, G. Li, W. M. Du, R. M. Pick, and C. Dreyfus, Phys. Rev. E **55**, 1232 (1997).

[23] D. R. Bauer, J. I. Brauman, and R. Pecora, Annu. Rev. Phys. Chem. **27**, 443 (1976).

[24] B. J. Berne and R. Pecora, *Dynamic Light Scattering: With Applications to Chemistry, Biology, and Physics* (Dover, Mineola, NY, 2000).

[25] A. Brodin, R. Bergman, J. Mattsson, and E. A. Rössler, Eur. Phys. J. B **36**, 349 (2003).

[26] J. C. Dyre, J. Phys. C **19**, 5655 (1986).

[27] J. C. Dyre, J. Appl. Phys. **64**, 2456 (1988).

[28] F. S. Howell, R. A. Bose, P. B. Macedo, and C. T. Moynihan, J. Phys. Chem. **78**, 639 (1974).

[29] J. R. Sangoro, C. Iacob, A. Serghei, C. Friedrich, and F. Kremer, PhysChemChemPhys **11**, 913 (2009).

[30] R. Richert, A. Agapov, and A. P. Sokolov, J. Chem. Phys. **134**, 104508 (2011).

[31] C. Iacob, J. R. Sangoro, A. Serghei, S. Naumov, Y. Korth, J. Karger, C. Friedrich, and F. Kremer, J. Chem. Phys. **129**, 234511 (2008).

[32] J. R. Sangoro, A. Serghei, S. Naumov, P. Galvosas, J. Karger, C. Wespe, F. Bordusa, and F. Kremer, Phys. Rev. E **77**, 051202 (2008).

[33] L. Pauling, *The Nature of the Chemical Bond and the Structure of Molecules and Crystals: An Introduction to Modern Structural Chemistry* (Cornell University Press, Ithaca, NY, 1960).

[34] H. Tokuda, K. Hayamizu, K. Ishii, M. Abu Bin Hasan Susan, and M. Watanabe, J. Phys. Chem. B **108**, 16593 (2004).

[35] R. Bohmer and C. A. Angell, Phys. Rev. B **45**, 10091 (1992).

[36] H. Tokuda, K. Hayamizu, K. Ishii, M. A. B. H. Susan, and M. Watanabe, J. Phys. Chem. B **109**, 6103 (2005).

[37] H. Tokuda, K. Ishii, M. A. B. H. Susan, S. Tsuzuki, K. Hayamizu, and M. Watanabe, J. Phys. Chem. B **110**, 2833 (2006).

[38] J. E. Mark, *Physical Properties of Polymers Handbook* (AIP, Woodbury, NY, 1996).

[39] J. Dudowicz, K. F. Freed, and J. F. Douglas, J. Chem. Phys. **124**, 064901 (2006).

[40] S. F. Swallen, P. A. Bonvallet, R. J. McMahon, and M. D. Ediger, Phys. Rev. Lett. **90**, 015901 (2003).

[41] M. K. Mapes, S. F. Swallen, and M. D. Ediger, J. Phys. Chem. B **110**, 507 (2006).

[42] I. Chang, F. Fujara, B. Geil, G. Heuberger, T. Mangel, and H. Sillescu, J. Non-Cryst. Solids **172**, 248 (1994).

[43] S. F. Swallen, K. Traynor, R. J. McMahon, M. D. Ediger, and T. E. Mates, J. Phys. Chem. B **113**, 4600 (2009).

[44] N. Ito and R. Richert, J. Phys. Chem. B **111**, 5016 (2007).

[45] K. S. Schweizer and E. J. Saltzman, J. Phys. Chem. B **108**, 19729 (2004).

[46] X. Y. Xia and P. G. Wolynes, Phys. Rev. Lett. **86**, 5526 (2001).

[47] R. Richert, J. Chem. Phys. **123**, 154502 (2005).

[48] R. Richert, K. Duvvuri, and L. T. Duong, J. Chem. Phys. **118**, 1828 (2003).

[49] D. L. Sidebottom and C. M. Sorensen, J. Chem. Phys. **91**, 7153 (1989).

[50] N. Petzold and E. A. Rössler, J. Chem. Phys. **133**, 124512 (2010).

[51] G. Li, W. M. Du, X. K. Chen, H. Z. Cummins, and N. J. Tao, Phys. Rev. A **45**, 3867 (1992).

[52] F. Stickel, E. W. Fischer, and R. Richert, J. Chem. Phys. **102**, 6251 (1995).

[53] F. Stickel, E. W. Fischer, and R. Richert, J. Chem. Phys. **104**, 2043 (1996).

[54] R. Casalini, K. L. Ngai, and C. M. Roland, Phys. Rev. B **68**, 014201 (2003).

[55] J. Thar, M. Brehm, A. P. Seitsonen, and B. Kirchner, J. Phys. Chem. B **113**, 15129 (2009).

[56] V. Kempter and B. Kirchner, J. Mol. Struct. **972**, 22 (2010).

[57] M. Kohagen *et al.*, J. Phys. Chem. B **115**, 15280 (2011).